CHEMISTRY OF MATERIALS

Article

pubs.acs.org/cm

InP Nanocrystals with Color-Tunable Luminescence by Microwave-Assisted Ionic-Liquid Etching

Raghavender Siramdas and Emily J. McLaurin*

Department of Chemistry, Kansas State University, 213 Chemistry and Biochemistry Building, 1212 Mid-Campus Drive North, Manhattan, Kansas 66506, United States

Supporting Information

ABSTRACT: This article reports the successful synthesis of luminescent InP nanocrystals (NCs) of different sizes using microwave-assisted methods. The key to NC photoluminescence (PL) is the use of 1-butyl-4-methylpyridinium tetrafluoroborate (BMPy BF_4), an ionic liquid (IL) with a fluoride-containing anion. The IL is responsible for both rapid heating of the reaction solution and efficient PL from the NCs. This is demonstrated by comparison with other ionic liquids, an analogous synthesis done using a flask and heating mantle, and a microwave-assisted synthesis in a silicon carbide (SiC) vessel. Addition of amine results in InP NC sizes ranging from ~3.2−4.2 nm, calculated (PL from ~545−630 nm) with quantum yields (QYs) of up to 30% and PL full-width-at-half-max (fwhm) values as small as ~0.18 eV (~59 at 632 nm) without optimization. By taking advantage of efficient microwave-assisted heating, this simple procedure provides a pathway to luminescent InP NCs of different diameters without changing precursors, performing sequential additions of reactants, or other postreaction processing (e.g., shell growth, HF etching).

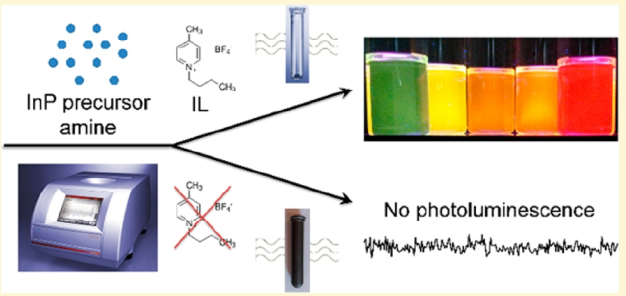

INTRODUCTION

The popularity of colloidal semiconductor nanocrystals (NCs) can be attributed to their use in electronic[1−3] and biological[4−6] technologies as well as the fundamental interest in their physical and chemical properties.[7,8] Related to the latter, interest in their surfaces has grown due to the large effect small changes in surface composition and structure have on NC behavior and capabilities.[9] Understanding and controlling these surfaces is an enticing area for chemists. Unfortunately, the best materials for these applications are often heavy metal-containing materials, such as CdSe and PbS, whose toxicity provides a barrier to growth of NC usage.[10−12]

One alternative is III−V semiconductors, which are ubiquitous in bulk technologies.[13,14] NCs of these materials have proven challenging to reproducibly synthesize with high quality (quantum yield, narrow size-distribution).[15,16] In particular, InP NCs exhibit luminescence in the visible range but have poor tunability with respect to NC size and, thus, optical properties. Unlike syntheses of II−VI nanocrystals, InP syntheses frequently require different precursors to obtain different sizes.[17,18] Alternatively, changing ratios of ligands or sequential additions of precursors can be used to obtain InP NCs with different diameters.[17,19] More recently, reaction temperature was used to tune InP NC size,[20,21] but despite these and other recent advances in InP NC synthesis,[22−29] postreaction processing is generally required to obtain luminescent InP NCs.

The two most popular techniques for obtaining luminescent InP NCs are 1) addition of shells to InP cores[30] and 2) etching using HF.[31−33] Shells are frequently ZnS, or related materials, and can be generated in single-step syntheses.[34−38] A recent report demonstrated addition of shells to InP cores results in QYs of up to 79%.[39] HF etching achieves quantum yields of more than 50%.[40] The mechanism for etching is hypothesized to involve removal of surface P vacancies (electron traps)[41] and activation of surface P dangling bonds (hole traps) for attack by fluoride.[31] Despite these advances, additional synthetic steps or modifications to InP NC cores are often problematic. Addition of shells can prevent transfer of charge-carriers from the NCs, which hinders many electronic applications.[42,43] Etching is associated with removal of native NC surface ligands or ligand-stripping,[44] a process that can improve NC charge transfer,[45] but it can also change the size of the NCs.[23,31,33] The use of HF is also dangerous as it is both highly corrosive and a contact poison.[46,47]

Although there are many examples of microwave-assisted synthesis of NCs in the literature, there is a strong bias toward metal and oxide nanoparticles prepared in polar solvent.[48−50] For other II−VI NCs and III−V NCs, colloidal preparations often involve high-boiling, hydrophobic solvents, and ligands.[51−53] These solvents allow for reaction at high temperature to obtain higher quality, more crystalline NCs. For microwave-assisted NC syntheses they highlight a key issue with the use of this synthetic method: a material with a good

Received: October 18, 2016
Revised: February 15, 2017
Published: February 15, 2017

DOI: 10.1021/acs.chemmater.6b04457
Chem. Mater. 2017, 29, 2101−2109

microwave dissipation factor (loss tangent) is required for heating.[54] In the absence of polar solvent, heating is achieved either through the reactants or the reaction vessel (usually glass). This can lead to very slow heating rates and, often, large size distributions.[53,55]

One way to increase heating rates in microwave-assisted syntheses is the addition of ionic liquids (ILs). ILs have low melting points but are not necessarily liquid at room temperature.[56] Their ionic nature makes them ideal for microwave-assisted syntheses as ionic conduction can markedly increase heating rates.[54] The microwave-assisted ionic-liquid (MAIL) method uses ILs in conjunction with organic solvents to promote rapid microwave heating.[57−59] The ILs couple well with microwaves and efficiently dissipate microwave energy as heat. As with any additive, the IL can interfere with the synthesis itself, and a less intrusive heating method may be desired.[60] One well-established process is microwave-assisted decomposition of ILs with fluoride-containing anions.[61] Even though it is not always desirable,[62] IL fluoride release was used to successfully synthesize fluoridic nanomaterials,[63] and nearly a decade ago, luminescent InP NCs were obtained using MAIL decomposition.[64] In the procedure developed by Strouse and co-workers, ILs and related fluoride-containing salts were combined with an InP precursor and rapidly heated in a microwave reactor to obtain NCs. The NCs had diameters of 2.7 ± 0.3 nm and QYs approaching 50%, which changed with the amount and composition of IL. The method was also used to form luminescent InGaP NCs,[65] but despite its success and simplicity, it has not been popularized. To the best of our knowledge there are no subsequent literature reports of its use for luminescent InP NC formation.

Here, we report expansion of this work to obtain luminescent shell-free InP NCs of different sizes. By varying the reaction temperature and microwave set-power (SP) and adding amine, the NC diameter could be tuned from 3.2 to 4.2 nm calculated corresponding to PL ranging from green to red with quantum yields of up to 30% without optimization. By investigating microwave powers up to 800 W, much larger than the commonly used maximum of 300 W, we obtain insight into the interplay between MAIL heating and NC formation. The NC growth and possible processes that lead to luminescent InP NCs were investigated by performing syntheses in the presence or absence of amine and IL. A silicon carbide (SiC) vessel was used to help mimic convective heating methods, and comparison with a conventional reaction done using an analogous procedure provides insight into the real advantages of microwave reactors for NC synthesis.

■ RESULTS AND DISCUSSION

The microwave-assisted method presented here is key to the luminescent InP NC synthesis. Two specific advantages over conventional heating are 1) the use of a solvent at elevated pressures and 2) selective heating of the IL. The first is one of the known advantages of microwave reactors (or other pressurized methods) and can provide enhanced reaction rates.[66] Here, decane was chosen as the solvent to enhance microwave interactions with the IL and increase the reaction speed. We expect the reaction to go faster at the elevated pressures (20 bar) reached in the solvent, and decane is more readily separated from the NCs than oily alternatives such as octadecene.[67] Second, decane provides a "window" for the microwaves, as it has little coupling with the field, allowing the waves to interact with the IL and "selectively heat".

Here, we exploit the IL for heating and as a reactant. As reactants, the ILs with BF_4^- anions decompose to release fluoride. Although the mechanism of release was not studied, subsequent etching is similar to processes associated with etching of bulk semiconductor surfaces.[68,69] These methods can leave fluoride on the semiconductor surfaces and previous MAIL etching of InP NCs confirmed the presence of fluorine using ^{19}F MAS NMR.[64] In conjunction with release of fluoride, the corresponding neutral halide (BF_3) forms. This quintessential Lewis acid is used for removal of native ligands from NC surfaces, so-called ligand stripping. Recent work using PbSe and BF_3:Et_2O demonstrated an elegant mechanistic pathway for this ligand-stripping process, which forms "naked" NCs.[44] The native PbSe oleate ligands are "stripped", ultimately forming BF_4^- and $OA_x(B_yF_z)$ byproducts and cationic NCs, which can be well dispersed in polar solvent such as DMF. Thus, using these BF_4^--containing ILs as reactants can modify the NC surfaces in multiple ways.

Luminescent InP NCs by *In Situ* Etching. The general procedure used for InP NC synthesis was adapted from the work of Lovingood and Strouse.[64] A simplified procedure is shown in Scheme 1. Briefly, an "InP" precursor is synthesized

Scheme 1. Microwave-Assisted Synthesis of InP NCs

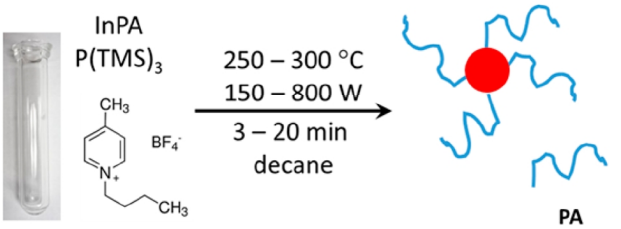

using InPA and $P(TMS)_3$. After heating the mixture in decane to obtain a clear solution, InP NCs are synthesized by combining the IL and precursor in an inert atmosphere in a Pyrex vessel. The vessel is then heated in a microwave reactor, while stirring. The precursor must be used immediately after preparation to obtain high quality NCs reproducibly. Variations in products were observed for reactions done at different temperatures, times, and SPs. Initially, the SP of the microwave was changed to assess the effect of microwaves on the synthesis, as previous experiments were limited to 300 W SP.[64] The effect of microwave SP is examined with respect to heating rate and reaction temperature. This effect is best demonstrated with a high (800 W) and low (150 W) SP. Plots of power and temperature vs time are shown in Figure 1. At the high SP (Figure 1A), the microwave applies the full 800 W to the solution for less than 5 s before decreasing the power to prevent overheating and modulating the power to maintain a temperature of 297 ± 3 °C. This results in power oscillations of about 200 W and a ramp time of ∼100 s. The total reaction time is thus ∼16.5 min (plus ∼5 min cooling time). In contrast, low SP (Figure 1B) requires the reactor to apply the maximum power for more than 5 min before dropping. Oscillations of 150 W maintain the reaction temperature of 295 ± 4 °C. The ramp time jumps to 6 min, with a total reaction time of ∼21 min (plus ∼5 min cooling). At SPs between 150 and 800 W SP, temperature vs time plots similar to these are observed, but the oscillations in power remain ≤450 W for all SPs (Figure S1). Thus, the 150 W SP provides a limiting heating condition for comparison to a higher, 800 W SP.

DOI: 10.1021/acs.chemmater.6b04457
Chem. Mater. 2017, 29, 2101−2109

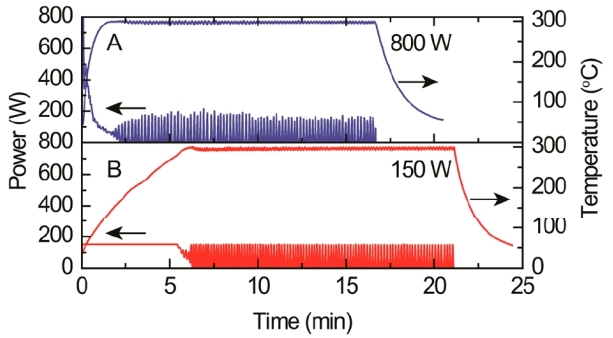

Figure 1. Power and temperature vs time plots. (A) At the high set-power (SP) extreme, 800 W power is applied for <5 s and oscillates nearly 200 W to maintain the set-temperature of 300 °C. This results in a ramp time of <2 min and a total reaction time of ~16.5 min plus ~5 min cooling. (B) At low SP, 150 W power is applied to the solution for >5 min before dropping. A ramp time of 6 min is required to reach 300 °C, and a total reaction time of 21 min plus 5 min cooling is required. The oscillations are limited to the SP of 150 W.

By comparing the photophysical properties of the NCs prepared at different temperatures and SPs, the effect of reaction conditions at high and low power can be parsed out. Figure 2 shows the absorption and PL spectra of InP NCs prepared at the 800 and 150 W SPs. The reaction temperature was varied to obtain different sizes, as was demonstrated recently by Xie et al.[25] Based on the absorption spectra, there is a small increase in size with increasing temperature. At 150 W SP and 250 °C, the smallest NCs form, as indicated by the first absorption feature near 500 nm and PL peak near 550 nm. The PL of this sample is low (QY < 3%), and the broad shoulder at lower energy is indicative of poorly defined surfaces (surface defects).[70] This shoulder decreases as the reaction temperature increases from 250 to 300 °C. This is true for the NCs prepared at a SP of 800 W as well, but the shoulder is not as prominent. The 800 W samples exhibit a noticeable broadening in their absorption feature at reaction temperatures ≥270 °C. This is likely due to a broad size-distribution and was observed with postsynthetic HF etching of InP NCs as well.[40,65] The PL full-width at half-maximum (fwhm) values also suggest a broader

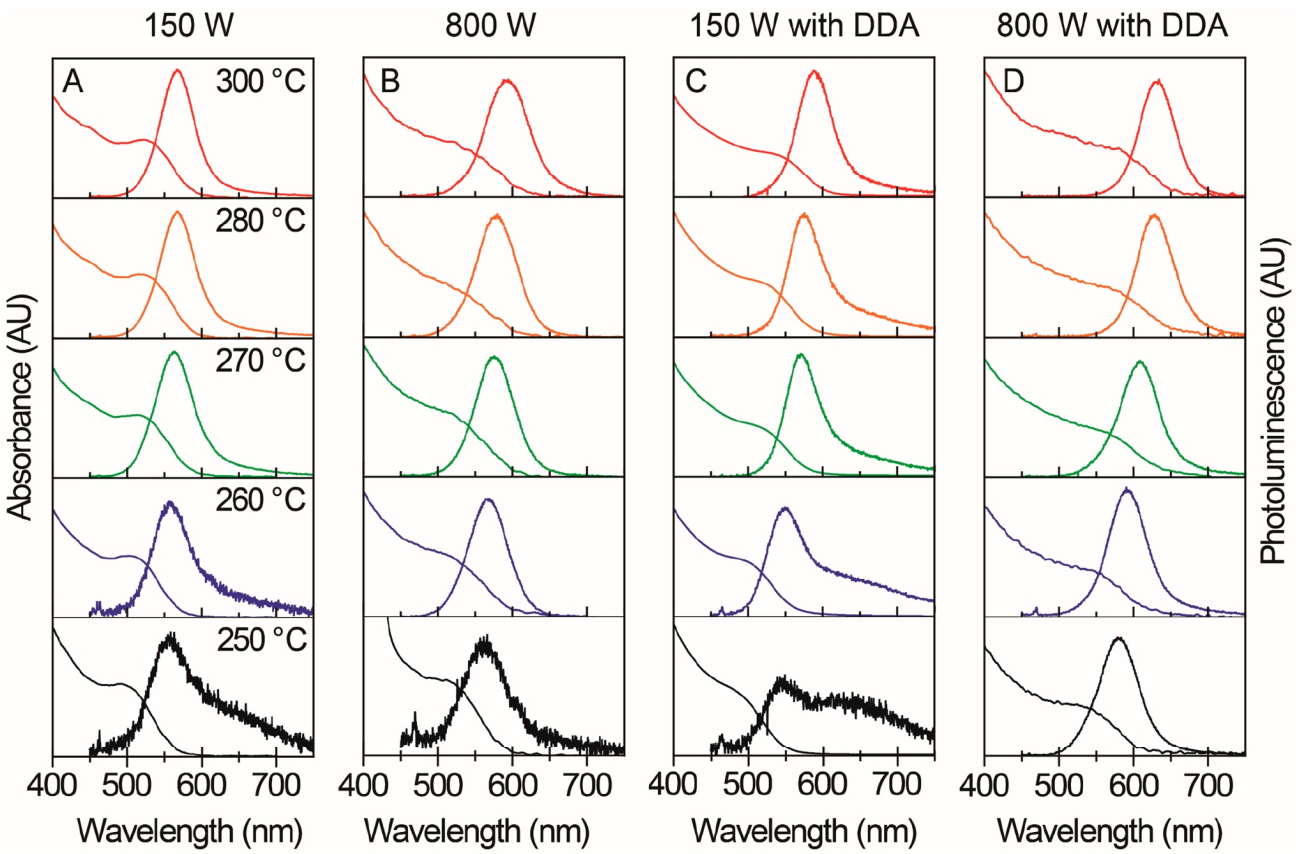

Figure 2. Absorption and photoluminescence (PL) spectra of InP NCs. (A) InP NCs prepared with 150 W set-power (SP) at 250 °C, 260 °C, 270 °C, 280 °C, and 300 °C. The InP PL is low at lower reaction temperatures and has a shoulder at lower energy, likely due to surface defects. The first absorption feature shifts from 497 to 522 nm, and the PL peak shifts from 553 nm to 574, indicating an overall increase in calculated diameter of 0.26 nm. (B) InP NCs prepared with 800 W SP at 250 °C, 260 °C, 270 °C, 280 °C, and 300 °C. The InP PL is low at 250 °C reaction temperature. The first absorption feature shifts from 508 to 528 nm, and the PL peak shifts from 562 to 596 nm indicating an overall increase in calculated diameter of 0.25 nm. (C) InP NCs prepared with 150 W SP with dodecylamine (DDA) at 250 °C, 260 °C, 270 °C, 280 °C, and 300 °C. The InP PL is low at lower temperatures, especially at 250 °C, with a broad shoulder. As temperature increases, the shoulder decreases, indicating an increase in surface passivation, and a red-shift in the PL and absorption peak are observed. The first absorption feature shifts from 484 to 529 nm, and the PL peak shifts from 544 nm to 588 indicating an overall increase in calculated diameter of 0.56 nm. (D) InP NCs prepared with 800 W SP with DDA at 250 °C, 260 °C, 270 °C, 280 °C, and 300 °C. As temperature increases, the first absorption feature shifts from 534 to 578 nm, and the PL peak shifts from 578 to 632 nm, indicating an overall increase in calculated diameter of 0.33 nm.

DOI: 10.1021/acs.chemmater.6b04457
Chem. Mater. 2017, 29, 2101−2109

size distribution for the samples prepared at 800 W and temperatures ≥270 °C with values of 0.25 ± 0.1 eV (69 ± 4 nm) vs 0.23 ± 0.1 eV (60 nm ±3 nm) for the samples prepared at 150 W and temperatures ≥270 °C. Low-resolution transmission electron microscopy (TEM) on samples indicates the NCs are spherical in shape (Figures S2−S3) and confirms a small overall increase in diameter for these samples. Sample aggregation made size-distribution determination a challenge, but, in general, larger distributions were obtained for larger NCs. These samples were prepared at higher temperatures requiring longer overall heating times, which can cause size broadening. Despite their broad absorption spectra, QYs were higher for the 800 W samples prepared at higher temperatures with values of 15 ± 5% vs <10% for the 150 W SP samples.

To further examine the effects of limiting reaction power, the synthesis was done with different hold times. As opposed to a hold time of 15 min at the reaction temperature, times were varied from 0 to 15 min at 280 °C. Absorption and PL spectra are shown in Figure S4. Only a small shift in the first absorption feature is observed, as it increases from ∼505 nm at 0 min to ∼525 nm at 15 min. A more interesting effect is present in the luminescence spectra. At short reaction times, very little or no luminescence is observed from the NCs. After 5 min hold time a defined PL peak is observed, increasing in intensity at 10 and 15 min hold times. This, along with the luminescence from samples prepared without amine (Figure 2A and 2B), suggests higher temperatures are required to obtain luminescent InP NCs because IL decomposition and related etching processes are known to occur at higher temperatures.[71]

The etching process affects the NC properties in multiple ways. To determine effects not realized by examination of their photophysical properties, further characterization was done using ^{1}H and ^{19}F NMR. Figure S5 shows the ^{1}H NMR spectrum of an InP NC sample prepared at high power and temperature. The presence of palmitate ligands associated with the NC surface is indicated by the broad peaks centered at 1.6 and 2.3 ppm, corresponding to the hydrogens nearest to the NC surface. The ^{19}F NMR spectra on these reaction products did not show any new peaks, despite analysis of many reactions. An example spectrum is shown in Figure S6 along with spectra of the IL alone and heated with and without palmitic acid. All of these spectra show strong peaks centered at −152 ppm with a 1:4 integrated intensity ratio, corresponding to BF_4^-. No other fluorine-containing species from the reactions were observed. Previously, ^{19}F MAS NMR on similar NCs indicated the presence of fluorine-containing species.[64] However, fluorine concentrations may be too low to observe here using solution techniques as signals associated with the NC surface are often broadened.[72]

In addition to the BMPy BF_4 IL, ILs with different cations and anions were utilized to assess the effects of the IL on the reaction and demonstrate the generality of the method. First, the analogous BMPy PF_6 IL was used. Although this IL did not yield luminescent InP NCs previously, employing lower temperatures and powers provided a pathway to luminescent InP NCs, as shown in Figure S7A. An IL with a more stable cation (BDMIm PF_6) could also successfully be exploited for luminescent InP NC synthesis (Figure S7B), although the NCs were not as bright (QYs < 10%). Finally, BMIm TFSI provided a fluoride-free IL control. Although NCs formed when using this IL, they did not luminesce (Figure S7C), suggesting a fluoride-containing anion is required for luminescent InP NCs. Assessing additional effects due to the IL is complicated by the different heating rates shown in the temperature vs time plots in Figure S8. The more lossy ILs heat the reaction solution more rapidly with BMIm TFSI > BMPy BF_4 > BDMIm PF_6 at 280 °C and 800 W. At 260 °C and 800 W, BMPy PF_6 resulted in faster heating than BMPy BF_4. Thus, the resulting InP NC products depend on the IL contribution to heating rate as well as the ability of the IL to influence the reaction chemically.

Microwave-Assisted Synthesis of Luminescent InP NCs with Amine. It is well-established that amines have an effect on InP NC formation.[27,28,73,74] A detailed study by Gary et al. found primary amines destabilized InP clusters, facilitating NC formation.[27] In more recent work, primary amines were shown to activate phosphorus precursors,[28,75] and Abolhasani et al. found the presence of amine increased the rate of nucleation of InP NCs.[26] Here, we add dodecylamine (DDA) to the microwave-assisted syntheses to obtain higher quality, larger InP NCs, examining the effects of power and temperature on the resulting NCs.

In general, InP NCs prepared with DDA were brighter and larger. Figure 2C and 2D show the absorption and PL spectra of InP NCs formed at temperatures ranging from 250 to 300 °C and 150 or 800 W SP in the presence of DDA. The highest QYs were obtained for NCs prepared at 300 °C (800 W, DDA) with a QY of 30%. In fact, the luminescence of samples prepared at 800 W with DDA is well-defined even for the sample prepared at 250 °C (Figure 2D). In Figure 2C a shoulder is observed in samples prepared at temperatures ≤260 °C with a very broad, lower energy emission present in the sample prepared at 250 °C. Samples prepared with DDA had absorption and PL peaks that could be tuned from ∼490 to ∼575 nm and ∼545 to ∼630 nm, respectively. This range is larger than that of samples prepared with no amine. These values are plotted along with the intermediate values obtained at different temperatures and in the absence of DDA in Figure 3. This plot shows the range of absorption peak and PL peak energies obtainable using this microwave-assisted method. It is readily apparent the samples prepared with DDA (triangles) show a larger range than those prepared without DDA (black squares and red circles). In fact, the DDA 150 W SP samples (green down-triangles) encompass the sizes obtainable with both 150 and 800 W in the absence of DDA.

The NC spectra varied slightly from synthesis-to-synthesis but consistently produced NCs with similar UV−vis absorptions and luminescence peak positions. Since amines provide the largest NC color-tunability, spectra for NCs synthesized using 150 and 800 W at 300 °C with amine were compared (Figure S9). Deviations in the first absorption feature were limited to ±5 nm (±0.02 eV) at 800 W and ±7 nm (±0.03 eV) at 150 W, likely due to the longer overall heating time required at lower powers. Corresponding PL spectra showed similar variations of ±7 nm (±0.02 eV) at 800 W and ±6 nm (±0.02 eV) and 150 W.

Overall, amine facilitates formation of larger, more red NCs stable for weeks. Using the first absorption feature, the diameters of the InP NCs were calculated, as described previously.[31,42] Calculated diameters ranging from 3.2 to 4.2 nm were obtained, and a plot of these values for samples prepared at different temperatures and powers is given in the SI (Figure S10). TEM images and XRD patterns for samples can also be found in the SI (Figure S11−S13). All samples exhibited spherical shape, and, in general, NC diameters increased with increasing temperature. TEM images confirm larger NCs form when amine is used in the reaction and a larger

DOI: 10.1021/acs.chemmater.6b04457
Chem. Mater. 2017, 29, 2101−2109

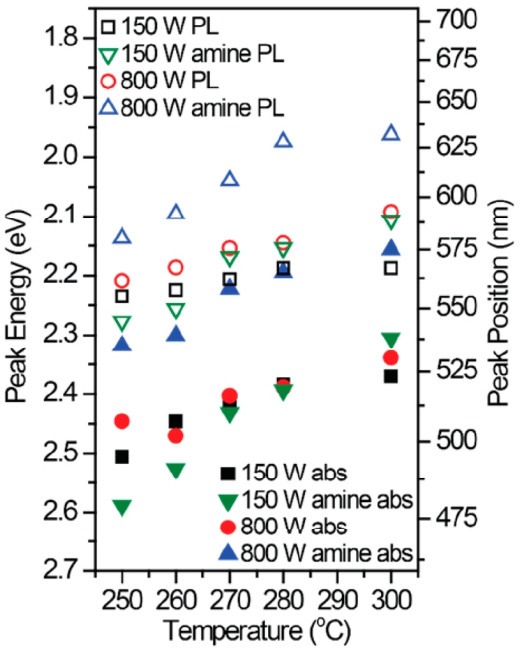

Figure 3. Scatter plot of absorption peak energy (eV) and PL peak position (nm) vs reaction temperature (°C). The degree of change in peak position is highest for the NCs prepared at 800 W set-power with amine, increasing from 578 to 632 nm (empty blue up-triangles). At 150 W with amine, the degree of increase in PL peak position is also high, ranging from 544 to 588 nm (empty green down-triangles). Without amine the magnitude of change in peak positions is lower at 800 and 150 W ranging from 562 to 596 nm and 553−574 nm, respectively.

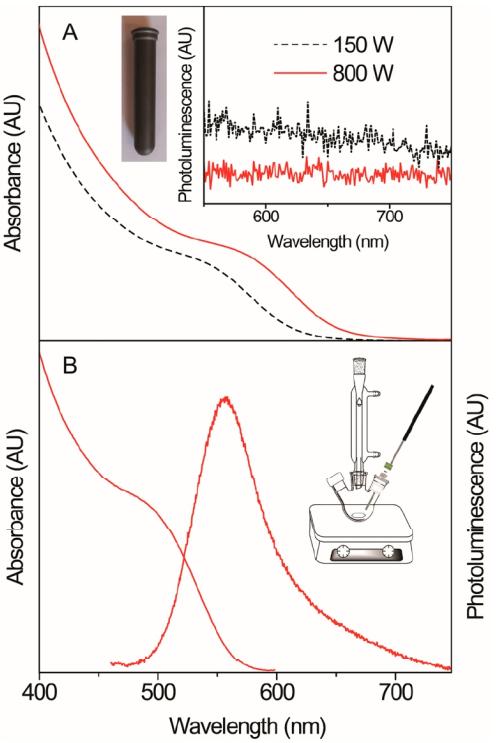

Figure 4. (A) UV−vis absorption spectra of InP NCs synthesized in a SiC vessel at 280 °C at set-powers (SPs) of 800 W (red, solid) and 150 W (black, dashed) in the absence of IL. The first absorption peak red-shifts from ∼530 nm to ∼570 nm as the SP changes from 150 to 800 W. In the SiC vessel, heating is predominantly due to convective heating, because there is no IL. The lack of IL also results in negligible NC luminescence (inset). (B) UV−vis absorption and photoluminescence spectra of InP NCs synthesized in a flask, which was heated to a reaction temperature of 280 °C with a holding time of 15 min. It took around 9 min to reach 280 °C. The PL shoulder indicates poor surface passivation, indicating that it is difficult to synthesize high-quality InP NCs, even at high temperatures (280 °C) in this conventional method.

size range is obtained. Size-distributions were similar for samples prepared at 150 and 800 W SP, with larger NCs exhibiting broader distributions, as observed with samples prepared with no amine. Although luminescence decreases over time, the NCs are stable in solution under ambient conditions for months. NCs prepared with amine and BMPy BF_4 IL exhibited luminescence after complete drying and exposure to air for 8 months, although the intensity decreased by ∼50% (Figure S14).

Microwave-Assisted Heating Without IL. To further examine the effects of amine on the synthesis, microwave-assisted syntheses were done without IL. However, the absence of IL is problematic due to slow heating rates. When no IL was used in the Pyrex vessel, the solution failed to reach the desired temperature (300 °C) despite heating as fast as possible at 800 W SP. This is likely due to poor coupling of the precursors to the microwave field, which is expected for these precursors. The dielectric constants of the precursors are 2.3 (palmitic acid), ∼3 (phosphine), 2 (decane), and 3.13 (DDA).[76,77]

To heat the solution rapidly in the absence of IL, a SiC vessel (Figure 4A inset) was used. The SiC vessel efficiently heats the reaction solution through convection, allowing rapid heating in the absence of IL and therefore separation of the effects of amine from the effects of IL on the synthesis.[60,78] The mixture reached reaction temperature (280 °C) in ∼3 min at 150 W and ∼2 min at 800 W (Figure S15). The resulting NCs exhibited no PL (Figure 4A inset), and the 150 W SP sample was noticeably smaller than the 800 W SP sample, as indicated by the first absorption features in Figure 4A. This is likely because of a discrepancy between internal and external temperature that is well-established in these microwave-assisted syntheses, including in SiC vessels.[60,78,79] Thus, at the higher SP, a higher internal temperature is reached for a longer time than at the lower 150 W SP. Here, the DDA causes a large size difference in the absence of the IL, indicating the size is predominantly a product of DDA and temperature, as previously observed for similar systems.[16,27,28]

Conventional Synthesis of InP NCs with IL. Finally, the effect of microwave heating on the reaction was examined by carrying out the synthesis using conventional methods. For this sample, an analogous procedure was followed. As opposed to combining the InP precursor and IL in a microwave vessel, they were combined in a flask fitted with a condenser, thermocouple, and septa, as shown in the Figure 4B, inset. The solution was heated to 280 °C using a heating mantle and temperature controller while stirring. Any effects related to microwave heating should be evident from differences between this and the standard MAIL synthesis. Specifically, possible etching related to IL decomposition should occur in the absence of microwaves because fluoride release is a thermal process.[61] The resulting NCs should exhibit luminescence straight out of the synthesis.

Absorption and PL spectra of the resulting NCs are shown in Figure 4B. The NCs exhibit PL but not as much as the NCs

DOI: 10.1021/acs.chemmater.6b04457
Chem. Mater. 2017, 29, 2101−2109

prepared at 800 W. The PL exhibits a shoulder to the red of the PL peak center, indicating the surface of the NCs may have more defects than other, more-etched NCs prepared in the microwave. For example, the InP NCs prepared at 280 °C and 800 W SP (Figure 2B) exhibit a PL peak centered at 578 nm with a fwhm of 67 nm (0.25 eV), and these NCs have a PL peak centered at 564 nm with a fwhm of 84 nm (0.34 eV). The first absorption feature is also quite broad, resembling that of other samples prepared in the absence of DDA.

Although not an exact comparison to the microwave-assisted method, largely because of the 9 min ramp time, the synthesis works in the absence of microwaves. Luminescence ascribed to IL fluoride release and related etching can still occur but does not seem as prominent as in the microwave-assisted syntheses, likely due to the higher T_{start} observed for slower heating rates.[71] Nevertheless, using this IL, it is possible to obtain luminescent InP NCs in the absence of microwaves, highlighting the thermal nature of the overall reaction.

Finally, we note that naked NCs form by stripping of oleate ligands from PbSe using BF_3:Et_2O.[44] Here, we generate BF_3 upon IL fluoride loss, and with native palmitate ligands, *in situ* ligand stripping can occur. However, the products obtained from these syntheses remain suspended in hydrophobic solvent, whereas cationic naked NCs can suspend in polar solvent, and peaks associated with bound palmitate were observed in ^{1}H NMR. Nevertheless, adjusting these initial reaction conditions could provide a pathway to yield an efficient *in situ* ligand-stripping agent and a new method for obtaining naked NCs.

■ CONCLUSIONS

In summary, we have investigated the effects of microwave power, reaction temperature, and amine on the microwave-assisted synthesis of InP NCs. Substantial differences in the heating profiles at different SPs and temperatures have been utilized to get InP NCs of different sizes. Although the magnitude of change in NC diameter is small at different SPs, addition of DDA facilitates a high degree of change in size at constant SP. This could be due to a combination of MAIL heating and precursor activation by amine, since brighter NCs form with DDA. Samples exhibited color-tunable luminescence spanning the visible region, with quantum yields of 20−30%. The IL role was assessed using ILs with different cations and anions, a SiC vessel, and a conventional flask synthesis, confirming ILs with fluoride-containing anions are largely responsible for 1) heating and 2) NC luminescence. However, the presence of fluoride on the NC surface was not observed. The effect of amine on size was confirmed using a SiC vessel in the absence of IL. The advantages of this microwave-assisted synthesis over conventional InP NC syntheses are its simplicity and that a single precursor solution yields luminescent InP NCs of different sizes.

■ EXPERIMENTAL SECTION

Materials. The following chemicals were used as received: indium acetate ($In(OAc)_3$, 99.99% trace metals basis), palmitic acid (PA, ≥99%), 1-butyl-4-methylpyridinium tetrafluoroborate (BMPy BF_4, ≥97%), 1-butyl-3-methylimidazolium bis(trifluoromethylsulfonyl)-imide (BMIm TFSI, ≥98%), 1-butyl-4-methylpyridinium hexafluorophosphate (BMPy PF_6, ≥97%), 1-butyl-2,3-dimethylimidazolium hexafluorophosphate (BDMIm PF_6, ≥97%), decane (≥99%), 1-octadecene (ODE, 90%), and dodecylamine (DDA, 98%) from Sigma-Aldrich; *tris*(trimethylsilyl)phosphine ($P(TMS)_3$), min. 98% (10% in hexane), and indium acetate ($In(OAc)_3$, 99.99%) from Strem; Fluorescein and Rhodamine B from Fisher Scientific; deuterated chloroform ($CDCl_3$) from Cambridge Isotope Laboratories.

Indium Palmitate (InPA). InPA was synthesized using a method adopted from Strouse and co-workers.[80] A 100 mL two-neck round-bottom (RB) flask was attached to a Schlenk line using a condenser; a rubber septum was attached, and the flask was put under vacuum. After filling the flask with N_2, 0.605 g (2.36 mmol) of PA was added. The solid was heated under vacuum while stirring in an oil bath at 105 °C for 5−10 min. After cooling the PA to room temperature under vacuum, the flask was put under N_2, and 0.207 g (0.710 mmol) of $In(OAc)_3$ was added. After putting the flask under vacuum, the solids were heated to 150 °C. Any solid that formed on the walls of the flask was melted using a heat gun. This process was repeated until the pressure reached baseline, about an hour. The flask was cooled to room temperature under vacuum, yielding a white solid.

InP Precursor. In an inert atmosphere glovebox, decane (47 mL) was added to the flask containing the InPA and left stirring until the solid was well-suspended (12 h). In the glovebox, $P(TMS)_3$ (1.15 mL, 0.393 mmol) was diluted in decane (3 mL) and slowly added to the InPA suspension. After obtaining an orange solution (1−2 h), the InP precursor solution was transferred to a Schlenk line and heated in an oil bath set to 65 °C under N_2. After the solution turned optically clear (~10 min), the flask was returned to the glovebox. The orange solution was immediately used as the precursor for the InP NC syntheses. This is essential for formation of high quality NCs reproducibly.

Microwave-Assisted InP NC Synthesis. The following methods were used for the synthesis of NCs. The ratio of InP precursor:IL was 1:10, and the ratio of InP precursor:DDA was 1:6. All samples were prepared in a glovebox under inert atmosphere in tightly capped 10 mL microwave vessels with a stir bar. The microwave method used the "heat as fast as possible" mode and a reaction time (holding time) of 15 min, unless otherwise indicated, followed by cooling to 55 °C using compressed air. After the microwave synthesis, the red/brown solution was separated from the dark-brown IL side product, which settled at the bottom, by a pipet. The sample was precipitated using acetone. The solid was isolated after centrifugation at 5100 rpm for 5 min and suspended in toluene. The precipitation and suspension (washing) procedures were repeated two more times, and the NCs were suspended in toluene for characterization.

Method I. InP precursor (3 mL) was combined with the ionic liquid (0.426 mmol) in a Pyrex microwave vessel. The vessel was capped, brought out of the glovebox, and put in the microwave reactor immediately. The mixture was heated to temperatures ranging from 250 to 300 °C at high (800 W) and low (150 W) set-powers (SPs).

Method II. InP precursor (3 mL) was added to BMPy BF_4 (82.5 μL) in a Pyrex microwave vessel followed by addition of DDA (0.046 g, 0.248 mmol). After the vessel was tightly capped, the mixture was stirred in the vessel for 3 min, brought out of the glovebox, and put in the microwave reactor immediately. The mixture was heated to temperatures ranging from 250 to 300 °C at 800 and 150 W SPs.

Method III. InP precursor (3 mL) was combined with DDA (0.046 g) in a silicon carbide (SiC) vessel. After tightly capping the vessel, the solution was stirred for 3 min, brought out of the glovebox, and immediately put in the microwave reactor. The mixture was heated to 280 °C at 800 or 150 W SP.

Conventional InP NC Synthesis. $In(OAc)_3$ (30.39 mg, 104.1 μmol) and PA (88.72 mg, 349.9 μmol) were combined in a 25 mL three-neck RB flask and heated to 150 °C. At this temperature, the RB flask was degassed for 20 min and then cooled to room temperature under vacuum. After taking the resulting white solid into a glovebox, 7.4 mL of a 7.73 mM solution of $P(TMS)_3$ in ODE was added to the RB flask. After 2 h of stirring, the mixture was transferred to a Schlenk flask and brought out of the glovebox to heat to 65 °C under N_2 gas supply in an oil bath. After obtaining an optically clear solution (InP precursor), the mixture was brought into a glovebox. To 3.7 mL of this InP precursor solution in a 20 mL three-neck RB flask was added 0.1 mL (0.51 mmol) of BMPy BF_4. The flask was brought out of the glovebox and attached to a Schlenk line through a condenser. After the RB flask was degassed for 20 min, it was heated to 300 °C using a

DOI: 10.1021/acs.chemmater.6b04457
Chem. Mater. 2017, 29, 2101−2109

thermocouple and temperature controller. It took 9.5 min to reach 300 °C. After heating at 300 °C for 15 min, the flask was cooled to room temperature. The resulting NC solution was washed with acetone and toluene 2 times, as described above.

Physical Measurements. Microwave syntheses were done using an Anton Paar Monowave 300 Microwave Reactor. In situ monitoring was accomplished using an IR sensor (for temperature) and a built-in camera (for changes in appearance). UV−vis absorption spectra were recorded with a Cary 500 or a Cary 5000 UV−vis-NIR spectrophotometer. Photoluminescence spectra were recorded using an Ocean Optics 2000+ spectrometer with 405 nm excitation or with a PTI Quanta Master 400 fluorometer. This fluorometer was also used for quantum yield measurements. Relative quantum yields of samples, Φ_{sam}, were calculated using Fluorescein and Rhodamine B in 0.1 N NaOH or water as the reference according to

$$\Phi_{sam} = \Phi_{ref}\left(\frac{A_{ref}}{A_{sam}}\right)\left(\frac{I_{sam}}{I_{ref}}\right)\left(\frac{\eta_{sam}}{\eta_{ref}}\right)^2$$

where A is the measured absorbance, η is the refractive index of the solvent, I is the integrated photoluminescence, and Φ_{ref} is the emission quantum yield of the reference. Φ_{ref} was taken to be 0.95 for Fluorescein in 0.1 N NaOH and 0.31 for Rhodamine B in water.[81,82] The first absorption features and PL peaks were fit to Gaussian distributions to determine their peak position and width. PL spectra were fit to two Gaussian distributions to represent trap emission, if present. For TEM analysis, a drop of sample was dried on a copper grid. TEM images were recorded using an FEI Tecnai G2 Spirit BioTWIN microscope. Powder X-ray diffraction (XRD) patterns were recorded by a Bruker D8 X-ray diffractometer or a PANalytical Empyrean multipurpose X-ray diffractometer. NMR spectra were recorded on Varian 400 MHz NMR in $CDCl_3$ solvent.

■ ASSOCIATED CONTENT

Supporting Information

The Supporting Information is available free of charge on the ACS Publications website at DOI: 10.1021/acs.chemmater.6b04457.

Plots of temperature and power vs reaction time, TEM images, UV−vis absorption, photoluminescence spectra, and NMR spectra (PDF)

■ AUTHOR INFORMATION

Corresponding Author

*E-mail: mclaurin@ksu.edu.

ORCID

Emily J. McLaurin: 0000-0002-7681-9587

Notes

The authors declare no competing financial interest.

■ ACKNOWLEDGMENTS

This research was supported by Kansas State University. This material is based upon work supported by the National Science Foundation under Grant No. CHE-1654793. TEM images were obtained through the Nanotechnology Innovation Center of Kansas State (NICKS). The authors thank M. Yazdanparast, S. Lee, and L. Beck for help with experiments.

■ REFERENCES

(1) Carey, G. H.; Abdelhady, A. L.; Ning, Z.; Thon, S. M.; Bakr, O. M.; Sargent, E. H. Colloidal Quantum Dot Solar Cells. *Chem. Rev.* **2015**, *115*, 12732−12763.

(2) Wood, V.; Bulović, V. Colloidal Quantum Dot Light-Emitting Devices. *Nano Rev.* **2010**, *1*, 5202.

(3) Yang, Y.; Zheng, Y.; Cao, W.; Titov, A.; Hyvonen, J.; Manders, J. R.; Xue, J.; Holloway, P. H.; Qian, L. High-Efficiency Light-Emitting Devices Based on Quantum Dots with Tailored Nanostructures. *Nat. Photonics* **2015**, *9*, 259−266.

(4) Frecker, T.; Bailey, D.; Arzeta-Ferrer, X.; McBride, J.; Rosenthal, S. J. Review—Quantum Dots and Their Application in Lighting, Displays, and Biology. *ECS J. Solid State Sci. Technol.* **2016**, *5*, R3019−R3031.

(5) Bruchez, M.; Moronne, M.; Gin, P.; Weiss, S.; Alivisatos, A. P. Semiconductor Nanocrystals as Fluorescent Biological Labels. *Science* **1998**, *281*, 2013−2016.

(6) Medintz, I. L.; Uyeda, H. T.; Goldman, E. R.; Mattoussi, H. Quantum Dot Bioconjugates for Imaging, Labelling and Sensing. *Nat. Mater.* **2005**, *4*, 435−446.

(7) Lifshitz, E.; Siebbeles, L. D. A. Fundamental Processes in Semiconductor Nanocrystals. *Phys. Chem. Chem. Phys.* **2014**, *16*, 25677−25678.

(8) Kovalenko, M. V.; Manna, L.; Cabot, A.; Hens, Z.; Talapin, D. V.; Kagan, C. R.; Klimov, V. I.; Rogach, A. L.; Reiss, P.; Milliron, D. J.; et al. Prospects of Nanoscience with Nanocrystals. *ACS Nano* **2015**, *9*, 1012−1057.

(9) Boles, M. A.; Ling, D.; Hyeon, T.; Talapin, D. V. The Surface Science of Nanocrystals. *Nat. Mater.* **2016**, *15*, 141−153.

(10) Rzigalinski, B. A.; Strobl, J. S. Cadmium-Containing Nanoparticles: Perspectives on Pharmacology and Toxicology of Quantum Dots. *Toxicol. Appl. Pharmacol.* **2009**, *238*, 280−288.

(11) Soenen, S. J.; Parak, W. J.; Rejman, J.; Manshian, B. (Intra)Cellular Stability of Inorganic Nanoparticles: Effects on Cytotoxicity, Particle Functionality, and Biomedical Applications. *Chem. Rev.* **2015**, *115*, 2109−2135.

(12) Grim, J. Q.; Manna, L.; Moreels, I. A Sustainable Future for Photonic Colloidal Nanocrystals. *Chem. Soc. Rev.* **2015**, *44*, 5897−5914.

(13) Cotal, H.; Fetzer, C.; Boisvert, J.; Kinsey, G.; King, R.; Hebert, P.; Yoon, H.; Karam, N. III−V Multijunction Solar Cells for Concentrating Photovoltaics. *Energy Environ. Sci.* **2009**, *2*, 174−192.

(14) Friedman, D. J. Progress and Challenges for next-Generation High-Efficiency Multijunction Solar Cells. *Curr. Opin. Solid State Mater. Sci.* **2010**, *14*, 131−138.

(15) van Veggel, F. C. J. M. Near-Infrared Quantum Dots and Their Delicate Synthesis, Challenging Characterization, and Exciting Potential Applications. *Chem. Mater.* **2014**, *26*, 111−122.

(16) Tamang, S.; Lincheneau, C.; Hermans, Y.; Jeong, S.; Reiss, P. Chemistry of InP Nanocrystal Syntheses. *Chem. Mater.* **2016**, *28*, 2491−2506.

(17) Xie, R.; Battaglia, D.; Peng, X. Colloidal InP Nanocrystals as Efficient Emitters Covering Blue to Near-Infrared. *J. Am. Chem. Soc.* **2007**, *129*, 15432−15433.

(18) Rowland, C. E.; Liu, W.; Hannah, D. C.; Chan, M. K. Y.; Talapin, D. V.; Schaller, R. D. Thermal Stability of Colloidal InP Nanocrystals: Small Inorganic Ligands Boost High-Temperature Photoluminescence. *ACS Nano* **2014**, *8*, 977−985.

(19) Xu, S.; Ziegler, J.; Nann, T. Rapid Synthesis of Highly Luminescent InP and InP/ZnS Nanocrystals. *J. Mater. Chem.* **2008**, *18*, 2653−2656.

(20) Baek, J.; Allen, P. M.; Bawendi, M. G.; Jensen, K. F. Investigation of Indium Phosphide Nanocrystal Synthesis Using a High-Temperature and High-Pressure Continuous Flow Microreactor. *Angew. Chem., Int. Ed.* **2011**, *50*, 627−630.

(21) Kim, K.; Yoo, D.; Choi, H.; Tamang, S.; Ko, J.-H.; Kim, S.; Kim, Y.-H.; Jeong, S. Halide−Amine Co-Passivated Indium Phosphide Colloidal Quantum Dots in Tetrahedral Shape. *Angew. Chem., Int. Ed.* **2016**, *55*, 3714−3718.

(22) Franke, D.; Harris, D. K.; Xie, L.; Jensen, K. F.; Bawendi, M. G. The Unexpected Influence of Precursor Conversion Rate in the Synthesis of III−V Quantum Dots. *Angew. Chem., Int. Ed.* **2015**, *54*, 14299−14303.

DOI: 10.1021/acs.chemmater.6b04457
Chem. Mater. 2017, 29, 2101−2109

(23) Mnoyan, A. N.; Kirakosyan, A. G.; Kim, H.; Jang, H. S.; Jeon, D. Y. Electrostatic Stabilized InP Colloidal Quantum Dots with High Photoluminescence Efficiency. *Langmuir* **2015**, *31*, 7117−7121.
(24) Tessier, M. D.; Dupont, D.; De Nolf, K.; De Roo, J.; Hens, Z. Economic and Size-Tunable Synthesis of InP/ZnE (E = S, Se) Colloidal Quantum Dots. *Chem. Mater.* **2015**, *27*, 4893−4898.
(25) Xie, L.; Harris, D. K.; Bawendi, M. G.; Jensen, K. F. Effect of Trace Water on the Growth of Indium Phosphide Quantum Dots. *Chem. Mater.* **2015**, *27*, 5058−5063.
(26) Abolhasani, M.; Coley, C. W.; Xie, L.; Chen, O.; Bawendi, M. G.; Jensen, K. F. Oscillatory Microprocessor for Growth and in Situ Characterization of Semiconductor Nanocrystals. *Chem. Mater.* **2015**, *27*, 6131−6138.
(27) Gary, D. C.; Terban, M. W.; Billinge, S. J. L.; Cossairt, B. M. Two-Step Nucleation and Growth of InP Quantum Dots via Magic-Sized Cluster Intermediates. *Chem. Mater.* **2015**, *27*, 1432−1441.
(28) Tessier, M. D.; De Nolf, K.; Dupont, D.; Sinnaeve, D.; De Roo, J.; Hens, Z. Aminophosphines: A Double Role in the Synthesis of Colloidal Indium Phosphide Quantum Dots. *J. Am. Chem. Soc.* **2016**, *138*, 5923−5929.
(29) Stein, J. L.; Mader, E. A.; Cossairt, B. M. Luminescent InP Quantum Dots with Tunable Emission by Post-Synthetic Modification with Lewis Acids. *J. Phys. Chem. Lett.* **2016**, *7*, 1315−1320.
(30) Mićić, O. I.; Smith, B. B.; Nozik, A. J. Core−Shell Quantum Dots of Lattice-Matched ZnCdSe2 Shells on InP Cores: Experiment and Theory. *J. Phys. Chem. B* **2000**, *104*, 12149−12156.
(31) Adam, S.; Talapin, D. V.; Borchert, H.; Lobo, A.; McGinley, C.; de Castro, A. R. B.; Haase, M.; Weller, H.; Möller, T. The Effect of Nanocrystal Surface Structure on the Luminescence Properties: Photoemission Study of HF-Etched InP Nanocrystals. *J. Chem. Phys.* **2005**, *123*, 084706.
(32) Mićić, O. I.; Cheong, H. M.; Fu, H.; Zunger, A.; Sprague, J. R.; Mascarenhas, A.; Nozik, A. J. Size-Dependent Spectroscopy of InP Quantum Dots. *J. Phys. Chem. B* **1997**, *101*, 4904−4912.
(33) Talapin, D. V.; Gaponik, N.; Borchert, H.; Rogach, A. L.; Haase, M.; Weller, H. Etching of Colloidal InP Nanocrystals with Fluorides: Photochemical Nature of the Process Resulting in High Photoluminescence Efficiency. *J. Phys. Chem. B* **2002**, *106*, 12659−12663.
(34) Li, L.; Reiss, P. One-Pot Synthesis of Highly Luminescent InP/ZnS Nanocrystals without Precursor Injection. *J. Am. Chem. Soc.* **2008**, *130*, 11588−11589.
(35) Lim, J.; Bae, W. K.; Lee, D.; Nam, M. K.; Jung, J.; Lee, C.; Char, K.; Lee, S. InP@ZnSeS, Core@Composition Gradient Shell Quantum Dots with Enhanced Stability. *Chem. Mater.* **2011**, *23*, 4459−4463.
(36) Kim, S.; Kim, T.; Kang, M.; Kwak, S. K.; Yoo, T. W.; Park, L. S.; Yang, I.; Hwang, S.; Lee, J. E.; Kim, S. K.; et al. Highly Luminescent InP/GaP/ZnS Nanocrystals and Their Application to White Light-Emitting Diodes. *J. Am. Chem. Soc.* **2012**, *134*, 3804−3809.
(37) Yang, X.; Zhao, D.; Leck, K. S.; Tan, S. T.; Tang, Y. X.; Zhao, J.; Demir, H. V.; Sun, X. W. Full Visible Range Covering InP/ZnS Nanocrystals with High Photometric Performance and Their Application to White Quantum Dot Light-Emitting Diodes. *Adv. Mater.* **2012**, *24*, 4180−4185.
(38) Wu, K.; Song, N.; Liu, Z.; Zhu, H.; Rodríguez-Córdoba, W.; Lian, T. Interfacial Charge Separation and Recombination in InP and Quasi-Type II InP/CdS Core/Shell Quantum Dot-Molecular Acceptor Complexes. *J. Phys. Chem. A* **2013**, *117*, 7561−7570.
(39) Altıntas, Y.; Talpur, M. Y.; Ünlü, M.; Mutlugün, E. Highly Efficient Cd-Free Alloyed Core/Shell Quantum Dots with Optimized Precursor Concentrations. *J. Phys. Chem. C* **2016**, *120*, 7885−7892.
(40) Li, C.; Ando, M.; Murase, N. Facile Preparation of Highly Luminescent InP Nanocrystals by a Solvothermal Route. *Chem. Lett.* **2008**, *37*, 856−857.
(41) Mićić, O. I.; Sprague, J.; Lu, Z.; Nozik, A. J. Highly Efficient Band-edge Emission from InP Quantum Dots. *Appl. Phys. Lett.* **1996**, *68*, 3150−3152.
(42) Reiss, P.; Protière, M.; Li, L. Core/Shell Semiconductor Nanocrystals. *Small* **2009**, *5*, 154−168.
(43) Smith, A. M.; Nie, S. Semiconductor Nanocrystals: Structure, Properties, and Band Gap Engineering. *Acc. Chem. Res.* **2010**, *43*, 190−200.
(44) Doris, S. E.; Lynch, J. J.; Li, C.; Wills, A. W.; Urban, J. J.; Helms, B. A. Mechanistic Insight into the Formation of Cationic Naked Nanocrystals Generated under Equilibrium Control. *J. Am. Chem. Soc.* **2014**, *136*, 15702−15710.
(45) Kagan, C. R.; Murray, C. B. Charge Transport in Strongly Coupled Quantum Dot Solids. *Nat. Nanotechnol.* **2015**, *10*, 1013−1026.
(46) MacKinnon, M. A. Hydrofluoric Acid Burns. *Dermatol. Clin.* **1988**, *6*, 67−74.
(47) Burgher, F.; Mathieu, L.; Lati, E.; Gasser, P.; Peno-Mazzarino, L.; Blomet, J.; Hall, A. H.; Maibach, H. I. Experimental 70% Hydrofluoric Acid Burns: Histological Observations in an Established Human Skin Explants Ex Vivo Model. *Cutaneous Ocul. Toxicol.* **2011**, *30*, 100−107.
(48) Baghbanzadeh, M.; Carbone, L.; Cozzoli, P. D.; Kappe, C. O. Microwave-Assisted Synthesis of Colloidal Inorganic Nanocrystals. *Angew. Chem., Int. Ed.* **2011**, *50*, 11312−11359.
(49) Horikoshi, S.; Serpone, N. Nanoparticle Synthesis through Microwave Heating. In *Microwaves in Nanoparticle Synthesis*; Horikoshi, S.; Serpone, N., Eds.; Wiley-VCH Verlag GmbH & Co. KGaA: Weinheim, Germany, 2013; pp 75−105.
(50) Zhu, Y.-J.; Chen, F. Microwave-Assisted Preparation of Inorganic Nanostructures in Liquid Phase. *Chem. Rev.* **2014**, *114*, 6462−6555.
(51) Murray, C. B.; Norris, D. J.; Bawendi, M. G. Synthesis and Characterization of Nearly Monodisperse CdE (E = Sulfur, Selenium, Tellurium) Semiconductor Nanocrystallites. *J. Am. Chem. Soc.* **1993**, *115*, 8706−8715.
(52) Mićić, O. I.; Curtis, C. J.; Jones, K. M.; Sprague, J. R.; Nozik, A. J. Synthesis and Characterization of InP Quantum Dots. *J. Phys. Chem.* **1994**, *98*, 4966−4969.
(53) van Embden, J.; Chesman, A. S. R.; Jasieniak, J. J. The Heat-Up Synthesis of Colloidal Nanocrystals. *Chem. Mater.* **2015**, *27*, 2246−2285.
(54) Gabriel, C.; Gabriel, S.; Grant, E. H.; Halstead, B. S. J.; Mingos, D. M. P. Dielectric Parameters Relevant to Microwave Dielectric Heating. *Chem. Soc. Rev.* **1998**, *27*, 213−224.
(55) Chikan, V.; McLaurin, E. J. Rapid Nanoparticle Synthesis by Magnetic and Microwave Heating. *Nanomaterials* **2016**, *6*, 85.
(56) Deetlefs, M.; Seddon, K. R. Ionic Liquids: Fact and Fiction. *Chim. Oggi* **2006**, *24*, 16.
(57) Liu, J.; Yang, X.; Wang, K.; Wang, D.; Zhang, P. Chemical Etching with Tetrafluoroborate: A Facile Method for Resizing of CdTe Nanocrystals under Mild Conditions. *Chem. Commun.* **2009**, 6080−6082.
(58) Hayakawa, Y.; Nonoguchi, Y.; Wu, H.-P.; Diau, E. W.-G.; Nakashima, T.; Kawai, T. Rapid Preparation of Highly Luminescent CdTe Nanocrystals in an Ionic Liquid via a Microwave-Assisted Process. *J. Mater. Chem.* **2011**, *21*, 8849−8853.
(59) Ma, M.-G.; Zhu, J.-F.; Zhu, Y.-J.; Sun, R.-C. The Microwave-Assisted Ionic-Liquid Method: A Promising Methodology in Nanomaterials. *Chem. - Asian J.* **2014**, *9*, 2378−2391.
(60) Kappe, C. O. Unraveling the Mysteries of Microwave Chemistry Using Silicon Carbide Reactor Technology. *Acc. Chem. Res.* **2013**, *46*, 1579−1587.
(61) Leadbeater, N. E.; Torenius, H. M. A Study of the Ionic Liquid Mediated Microwave Heating of Organic Solvents. *J. Org. Chem.* **2002**, *67*, 3145−3148.
(62) Hallett, J. P.; Welton, T. Room-Temperature Ionic Liquids: Solvents for Synthesis and Catalysis. *Chem. Rev.* **2011**, *111*, 3508−3576.
(63) Lorbeer, C.; Cybinska, J.; Mudring, A.-V. Facile Preparation of Quantum Cutting GdF3:Eu3+ Nanoparticles from Ionic Liquids. *Chem. Commun.* **2010**, *46*, 571−573.

DOI: 10.1021/acs.chemmater.6b04457
Chem. Mater. 2017, 29, 2101−2109

(64) Lovingood, D. D.; Strouse, G. F. Microwave Induced In-Situ Active Ion Etching of Growing InP Nanocrystals. *Nano Lett.* **2008**, *8*, 3394−3397.
(65) Gerbec, J. A. Methods of Synthesis of Colloidal Nanoparticles. Ph.D. Thesis, University of California, Santa Barbara: California, United States, 2006.
(66) Jhung, S. H.; Jin, T.; Hwang, Y. K.; Chang, J.-S. Microwave Effect in the Fast Synthesis of Microporous Materials: Which Stage Between Nucleation and Crystal Growth Is Accelerated by Microwave Irradiation? *Chem. - Eur. J.* **2007**, *13*, 4410−4417.
(67) Washington, A. L., II; Strouse, G. F. Microwave Synthesis of CdSe and CdTe Nanocrystals in Nonabsorbing Alkanes. *J. Am. Chem. Soc.* **2008**, *130*, 8916−8922.
(68) Bose, D. N.; Ramprakash, Y.; Basu, S. Characterization of N-InP Surfaces before and after Surface Modification. *Mater. Lett.* **1989**, *8*, 364−368.
(69) Sun, Y.; Liu, Z.; Machuca, F.; Pianetta, P.; Spicer, W. E. Optimized Cleaning Method for Producing Device Quality InP(100) Surfaces. *J. Appl. Phys.* **2005**, *97*, 124902.
(70) Fu, H.; Zunger, A. InP Quantum Dots: Electronic Structure, Surface Effects, and the Redshifted Emission. *Phys. Rev. B: Condens. Matter Mater. Phys.* **1997**, *56*, 1496−1508.
(71) Cao, Y.; Mu, T. Comprehensive Investigation on the Thermal Stability of 66 Ionic Liquids by Thermogravimetric Analysis. *Ind. Eng. Chem. Res.* **2014**, *53*, 8651−8664.
(72) Morris-Cohen, A. J.; Malicki, M.; Peterson, M. D.; Slavin, J. W. J.; Weiss, E. A. Chemical, Structural, and Quantitative Analysis of the Ligand Shells of Colloidal Quantum Dots. *Chem. Mater.* **2013**, *25*, 1155−1165.
(73) Protière, M.; Reiss, P. Amine-Induced Growth of an In2O3 Shell on Colloidal InP Nanocrystals. *Chem. Commun.* **2007**, 2417−2419.
(74) Allen, P. M.; Walker, B. J.; Bawendi, M. G. Mechanistic Insights into the Formation of InP Quantum Dots. *Angew. Chem.* **2010**, *122*, 772−774.
(75) Buffard, A.; Dreyfuss, S.; Nadal, B.; Heuclin, H.; Xu, X.; Patriarche, G.; Mézailles, N.; Dubertret, B. Mechanistic Insight and Optimization of InP Nanocrystals Synthesized with Aminophosphines. *Chem. Mater.* **2016**, *28*, 5925−5934.
(76) *Dielectric Constants Lookup Table*; Honeywell: Morris Plains, NJ, USA, 2010.
(77) *Dielectric Constant (DC Value) Compendium*; Endress+Hauser: Weil am Rhein, Germany, 2000.
(78) Ashley, B.; Lovingood, D. D.; Chiu, Y.-C.; Gao, H.; Owens, J.; Strouse, G. F. Specific Effects in Microwave Chemistry Explored through Reactor Vessel Design, Theory, and Spectroscopy. *Phys. Chem. Chem. Phys.* **2015**, *17*, 27317−27327.
(79) Kappe, C. O. How to Measure Reaction Temperature in Microwave-Heated Transformations. *Chem. Soc. Rev.* **2013**, *42*, 4977−4990.
(80) Gerbec, J. A.; Magana, D.; Washington, A.; Strouse, G. F. Microwave-Enhanced Reaction Rates for Nanoparticle Synthesis. *J. Am. Chem. Soc.* **2005**, *127*, 15791−15800.
(81) Magde, D.; Rojas, G. E.; Seybold, P. G. Solvent Dependence of the Fluorescence Lifetimes of Xanthene Dyes. *Photochem. Photobiol.* **1999**, *70*, 737−744.
(82) Magde, D.; Wong, R.; Seybold, P. G. Fluorescence Quantum Yields and Their Relation to Lifetimes of Rhodamine 6G and Fluorescein in Nine Solvents: Improved Absolute Standards for Quantum Yields. *Photochem. Photobiol.* **2002**, *75*, 327−334.

DOI: 10.1021/acs.chemmater.6b04457
Chem. Mater. 2017, 29, 2101−2109